ChemComm

Accepted Manuscript

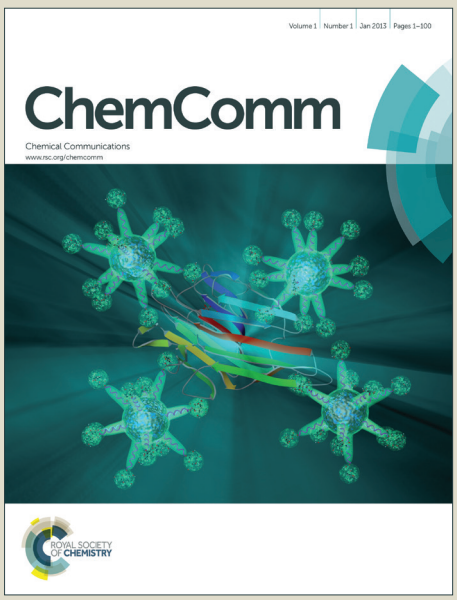

ROYAL SOCIETY OF CHEMISTRY

www.rsc.org/chemcomm

ChemComm

COMMUNICATION

The Beauty of Frost: Nano-Sulfur Assembly via Low Pressure Vapour Deposition

Received 00th January 20xx,
Accepted 00th January 20xx

DOI: 10.1039/x0xx00000x
www.rsc.org/

Yu Wang,*[a] Lu Chen,[a] Louis Scudiero,[b] and Wei-Hong Zhong*[a]

A low pressure vapour deposition (LPVD) technique is proposed as an environmentally friendly, cost-effective and versatile strategy for fabrication of sulfur nanomaterials. By controlling the characteristics of the deposite substrate for the LPVD, various sulfur-based nanomaterials have been achieved through a substrate-induced self-assembly process.

Introduction

Elemental sulfur is one of the most important elements on earth with broad application. Its abundance, environmentally friendly nature and significant chemical/electrochemical performance make it an advanced material in many fields, such as energy, medicines, construction, agriculture and so forth. In particular, sulfur is of great interest as a promising cathode material with high capacity for next generation batteries.[1-5] The theoretical capacity of sulfur cathode is around 1600 mAh/g, ca. 8 times the commercial cathodes.[6] Moreover, the high electrochemical reactivity of sulfur with various metals (e.g., Li, Na, Mg, or Al) lays the foundation for the studies on high-performance metal-sulfur batteries.[7] In addition to the important electrochemical properties, α-sulfur crystals were shown to possess semiconductor-like behaviour and can be used as a visible-light-active photocatalyst.[8, 9] In pharmaceutical area, sulfur has been used to treat acne and other kinds of inflammation of skin for thousands of years. For example, in Traditional Chinese Medicine sulfur was used for skin care even from BC era, which is about 2,200 years ago.

Consequently, technology for fabrication of nano-sulfur plays a critical role in further exploring the potentials of sulfur. For instance, nanostructured sulfur when used as an energy material can deliver a capacity close to its theoretical value and improve power density of the battery remarkably.[2, 10-12] By combining sulfur nanoparticles (S-NPs) with other functional nanomaterials, such as MoS2, the photocatalytic performance of the resulting hybrid was also found improved notably.[13] In biochemical applications, S-NPs have been reported as a green effective pesticide against various bacteria.[14, 15] In addition, the separation and concentration of some heavy metals in marine samples (eg. seawater, fish and oysters) have been also realized by hybrids of S-NPs and aluminum micro-particles.[16] However, it is noted that these nano-sulfur materials with significant properties for "green" technologies are conventionally produced by chemical approach. Among various chemical methods, deploying $Na_2S_2O_3$/acid represents the most classic one.[2, 17, 18] In this method, the nano-sulfur was either stabilized by surfactant or trapped by other nanomaterials introduced into the reaction systems. Other methods have also been reported. For example, S-NPs were generated from hazardous H_2S,[19] or produced by water-in-oil microemulsions technique,[20] or by a precipitation process from aqueous solutions.[21-23] It is noted that these methods either involve the use of solvents or the emission of toxic gases, such as H_2S and SO_2, which are not environmentally friendly and/or cost-effective. Therefore, developing resource-conserving, cost-effective and environmentally friendly fabrication technology for producing nano-sulfur and its nanohybrids is in critical need by the long-term success of sulfur and sulfur related materials.

In this communication, as shown in **Figure 1**, we report an exceptionally simple way, a Low Pressure Vapour Deposition (LPVD) method, for fast, solvent-free, toxic-gas-free and versatile fabrication of S-NPs and their assemblies. The fabrication process can be completed in a very short time, from several seconds to few minutes. Moreover, various assembly structures of the S-NPs with well-controlled morphology can also be achieved by controlling the surface characteristics of the

[a] School of Mechanical and Materials Engineering
[b] Department of Chemistry
Washington State University, Pullman, WA 99164
*Email: Katie_zhong@wsu.edu; yu.wang3@wsu.edu
Electronic Supplementary Information (ESI) available: [details of any supplementary information available should be included here]. See DOI: 10.1039/x0xx00000x

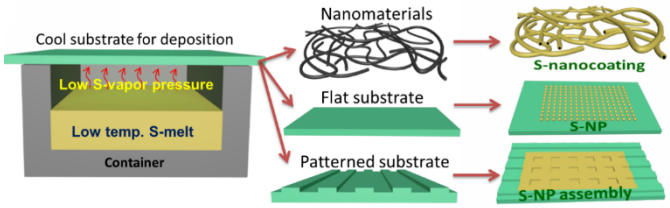

Fig. 1. Schematic of the Low pressure vapour deposition (LPVD) technique for fabrication of nano-sulfur. The temperature of sulfur melt is controlled in a low temperature range of 130 – 170 °C, which leads to a sulfur vapour pressure from 10 to 70 Pa (see Supporting Info. S1). The low sulfur vapour pressure provides an ideal condition for the growth of nano-sulfur on a cool substrate via physical vapour deposition. In addition, by adjusting the characteristics of the deposition substrate, various assembling structures of S can be achieved via a self-assembly process. For details, see the text.

deposition substrate. In specific, sulfur melt with low temperature from ca. 130 to 170 °C is employed for the LPVD. It is known that, at standard atmosphere the melting and boiling points of sulfur are ca. 115 °C and 445 °C, respectively. Therefore, compared to the boiling point, sulfur melt with a temperature within the range of 130 to 170 °C can be viewed as a low temperature sulfur melt for evapourating. Based on the data from the reference,[24] the sulfur vapour pressure, V_p, at different temperature can be determined (see Supporting Info. S1). For the temperature range mentioned above, the S-vapour pressure varies from 10 to 70 Pa, which is extremely low and usually cannot arouse any attention for potential application. However, in this study, the low V_p of sulfur melt was found to be exactly an ideal condition for the growth of S-NPs and S-assemblies as illustrated in Figure 1. The cool substrates (20 to 80 °C) act as nucleation "agent" and the S vapour can deposit and grow as S-NPs on the substrate surface. Due to the low vapour pressure, the deposition speed is self-controlled in a range suitable for the growth of S-NPs and S-assemblies. Moreover, when substrates with particular surface chemistry and morphology are used for the deposition, the S-NPs can further form different assemblies determined by the surface characteristics as shown below.

On flat substrate. Microscope cover glass was employed as a flat substrate for the deposition. The growing process of S-NPs on the glass substrate is illustrated in **Figure 2 (a).** From **Figure 2**, one can find that S-NPs can be produced via a LPVD process within only several seconds at a low temperature of 138 °C, that is, 11 Pa for sulfur vapour pressure. For the sample with 3-second deposition, the SEM images (**Figure 2 (b)** and Supporting Info. Figure S2 (A)) show that S-NPs formed in spherical shape with an average diameter of ca. 48 nm. The insert in **Figure 2 (b)** is the statistic result of the diameter distribution based on the measurement of 426 S-particles. It turns out there is ca. 80% of the S-NPs with a diameter in the range of 40 – 60 nm, indicating a narrow distribution of the particle size. After 10-second deposition, the S-NPs tend to form structures with rod-like morphology as shown in **Figure 2 (c)** and Supporting Info. Figure

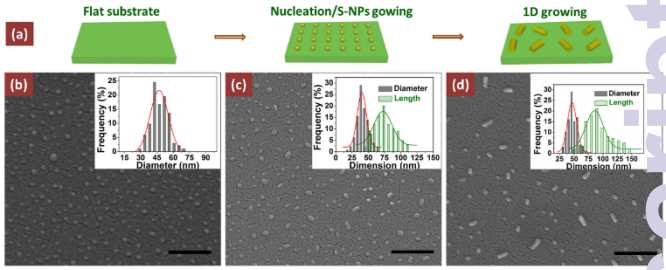

Fig. 2. Sulfur nanoparticles growing on a flat glass substrate via LPVD (a) Schematic of the growing process of S-NPs (the digital photo shows one glass with deposition of S-NPs for 60 s at 138 °C); SEM images of the S-NPs with different deposition time for 138 °C sulfur melt, (b) 3 s, (c) 10 s and (d) 60 s. The inserts are the statistic results of the size distribution of the S-NPs (Scale bars: 500 nm).

S2 (B). From the insert showing the statistic results of the diameter and length, one can find that the average diameter of the S-NPs (ca. 43 nm) doesn't change notably with increased deposition time; however, the S-NPs increase their volume by growing along one direction, which finally gives rise to the rod-like morphology. The average length for this 10-second deposition sample is ca. 74 nm, resulting in an aspect ratio (length/diameter) of 1.7. When the deposition time increased from 10 s to 60 s, the rod-like morphology becomes more obvious with an aspect ratio of 2.1 (see **Figure 2 (c)** and Supporting Info. Figure S2 (C)). Again, it can be found that the diameter (49 nm) maintains a value close to that for the previous sample with 3-second deposition. This self-controlling behaviour in the diameter indicates LPVD is a simple way to prepare S-NPs with well-controlled dimensions. It is noted that, in addition to the growth in the length direction, accumulation of S-NPs or re-melting of S-NPs can happen with increased deposition time, such as 60 seconds (see Supporting Info. Figure S2 (C)).

On one-dimensional NPs. In addition to the preparation of S-NPs, LPVD can also be employed for sulfur coating on other functional nano-materials. In this study, carbon nanofibers (CNFs) are employed for the demonstration. To obtain an effective S-coating, the surface chemistry of the nanomaterials was found very critical. In specific, a good affinity between sulfur vapour and the nanomaterials is a necessary precondition for the S-coating by LPVD. Due to the hydrophobic nature of elemental sulfur, a hydrophobic surface of nanomaterials will be in favour of a homogeneous deposition. The coating process of S-vapour by deposition on one-dimensional hydrophobic CNFs is shown by the schematic, **Figure 3 (a)**. In particular, the 1D nanomaterial CNF acts as an effective nucleation agent for the sulfur deposition. In this case, the high surface area of CNFs means a high density of nucleation point. With the further deposition of sulfur on each nucleus, the sulfur particle grows bigger and bigger, which finally results in the merging of adjacent sulfur particles along the same CNF. This process is very similar to that of the preparation of a popular traditional Chinese food, a stick of sugar-coated haws as shown in **Figure 3 (a)**.

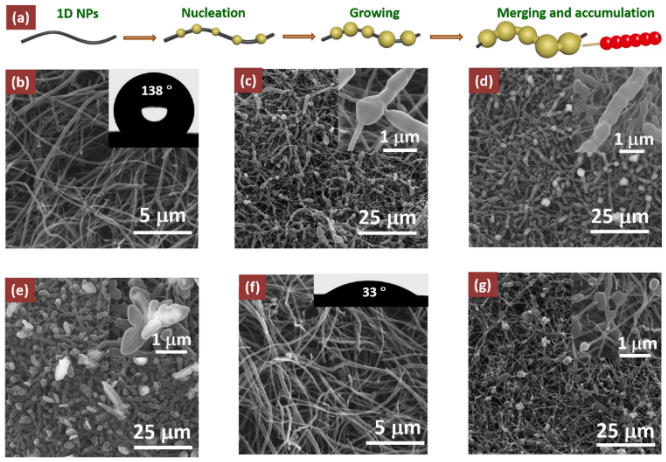

Fig. 3. Sulfur-based nanohybrids with one-dimensional conductive nanomaterials (eg. carbon nanofiber) by LPVD. (a) Schematic of the coating process; (b) SEM image of the pristine CNFs with hydrophobic surface (see the insert for the contact angle); (c) - (e), SEM images of the hydrophobic CNFs sample with different sulphur deposition time: 1 min., 3min. and 7 min. respectively; (f) SEM image of the SDS-treated CNFs with hydrophilic surface (also see the insert for the contact angle); (g), SEM images of the SDS-treated CNFs after 3 min. of sulfur deposition.

Indeed, when hydrophobic CNFs (See **Figure 3 (b)**) were employed, a coating layer of sulfur on the CNFs can be realized in few minutes by the LPVD. **Figure 3 (c) – (e)** show the deposition process at different times: 1 min., 3min. and 7 min. respectively. It can be found that there is an optimal deposition time for achieving a homogenous coating layer. A long deposition time, such as 7 min., with V_p of ca. 22 Pa., gave rise to extra sulfur deposition on the top of saturated CNF-sulfur hybrid as shown in **Figure 3 (e)**. While, for an insufficient deposition time, such 1 min., only part of the CNFs was coated by S-layer as displayed **Figure 3 (c)**. The S-coating layer on CNF is clearly shown by the inserted SEM image in **Figure 3 (c)**. Only, when an appropriate deposition time is applied, such as 3 min., one can obtain a homogeneous S-coating along the CNFs as shown in **Figure 3 (d)**. The resultant CNF-sulfur hybrid with the optimized deposition time displays worn-like morphology with a diameter of ca. 900 nm, indicating that there is a sulfur coating layer with about 350 nm in thickness if the diameter of the CNF core (ca. 200 nm) has been taken into consideration. Based on the XRD data (see Supporting Info. Figure S3), the deposited sulfur is α-sulfur of S_8, the most common and stable phase of sulfur. It is noted that the S-coating is mainly observed for the CNFs on the surface of the CNF-substrate due to the diffusion barrier inside the CNF-substrate. In contrast, when hydrophilic CNFs (controlled by the surfactant on the surface) were used as the substrate for the deposition, the sulfur vapour was not effectively deposited on the CNF surface owing to the poor affinity between hydrophilic CNFs and sulfur vapour (see **Figure 3 (f)** and **(g)**). The small amount of individual sulfur particles observed on the hydrophilic sample is probably related to some defects of the surfactant treatment or other unknown phenomena.

On patterned surface. Another significant finding about LPVD is the self-assembly behavior of nano-sulfur on a patterned surface. Here, a blank CD-ROM with a pattern surface as illustrated in **Figure 4 (a)** has been used as the pattern substrate (one can obtain the pattern surface of polycarbonate side by removing the reflective Al layer that is, the label layer). The characteristics of the pattern structures were characterized by SEM images and contact angle (Supporting Info. Figure S4). The results show that the width of the groove is 560 ± 40 nm, and the width of the ridge is 820 ± 50 nm. Also, the contact angle results reveal an anisotropic wetting behaviour of a water droplet on the pattern surface, that is, the surface shows much more hydrophobic behaviour in the direction perpendicular to the grooves than the direction along the grooves. **Figure 4 (a)** also illustrates the self-assembly process of sulfur on the pattern surface by LPVD. At the initial state, the sulfur vapour forms a coating layer on the surface of both grooves and ridges (also see Supporting Info. Figure S5), and then, due to possible complicated phenomenon (such as interference of vapour flow along the grooves or the anisotropic hydrophobic behaviour of the substrate), the sulfur vapour starts to form bridges in the grooves. As the width of the bridge growing, a sulfur lattice can be obtained.

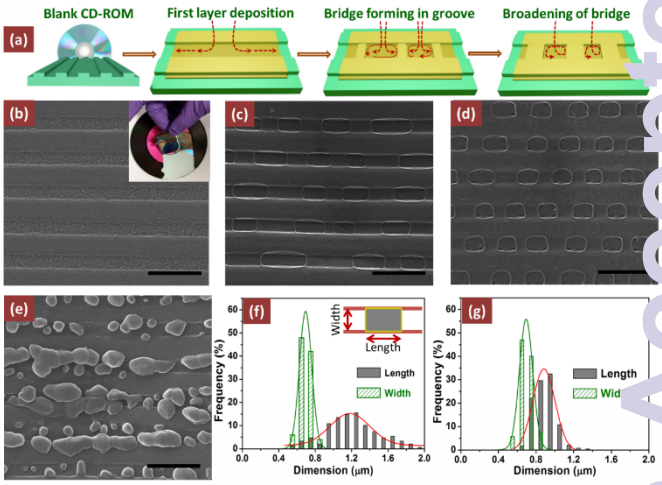

Fig. 4. Sulfur assembly on a patterned surface (eg. blank CD-ROM) by LPVD. (a) Schematic of the assembly process; (b) SEM image of the pattern surface of a blank CD-ROM before sulfur deposition (inset showing the peeling of the label layer to obtain the pattern surface); SEM images of the CD-ROM surface after sulfur deposition at different temperatures but with the same deposition time of 60 s: (c) 138 °C, (d) 150 °C, (e) 172 °C; (f) and (g), the statistic results of the dimensions of the square-like lattice assembly at 138 and 150 °C, respectively (Scale bars: 2 μm).

Figure 4 (b) is a typical SEM image displaying the groove-ridge repeating pattern surface of the blank CD-ROM. By deposition of sulfur at different temperature and with different deposition time, one can obtain a sulfur layer with various morphologies. Significantly, only for low temperature sulfur melt (e.g. 138 and 150 °C), one can achieve uniform lattice structures via sulfur assembly (see **Figure 4 (c) and (d),** and also Supporting Info. Figure S5 and S6). For a high

temperature sulfur melt (e.g., 172 °C) with vapour pressure of 67 Pa, it can be found that, instead of sulfur lattice, lots of big sulfur particles formed along the grooves as shown by **Figure 4 (e)** and Supporting Info. Figure S7. These results indicate that a high temperature sulfur melt or a high sulfur vapour pressure is not suitable for growing uniform and controllable S-NPs and sulfur assemblies. A further investigation on the effects of sulfur melt temperature on the sulfur assembly morphologies was performed by statistical analysis of the lattice structures. As summarized in **Figure 4 (f) and (g)**, the dimension in length of square-like pores of the lattice for the 138 °C sample is a little different from those for the 150 °C sample. In specific, the average length for 138 °C sample is 1.22 μm, while, it is 0.88 μm for 150 °C sample. At the same time, the distribution of the length for the 138 °C sample is much broader than that for the 150 °C sample. Moreover, it was also found that there is an obvious difference in the number density of the square-like pores: 4.6×10^5 mm^{-2} for 150 °C sample, 2.7×10^5 mm^{-2} for 138 °C sample. These differences should be related to the difference in sulfur vapour pressure. However, for the width of the square-like pores (660 nm for 138 °C sample, 690 nm for 150 °C), there is no significant difference since it is mainly controlled by the width of the grooves of the substrate (ca. 560 nm).

For a specific application of the LPVD technique described above, one can either separate the nanostructured sulfur from the substrate or keep it with the substrate. For example, one can remove the sulfur nanoparticles from the glass substrate by sonication in a suitable solvent. While, for the sulfur coating on CNF, it should be viewed as a hybrid nanomaterial, which can be directly used as a composite cathode for Lithium-sulfur battery or as active materials for catalytic application. For the pattern structure of nano-sulfur on the CD-ROM, one may keep the sulfur with the substrate as well and use it as a template. Clearly, these specific applications need more systematic studies, which is beyond the scope this study.

In summary, we have demonstrated the diversity of LPVD for fabrication of various sulfur nanomaterials. A low temperature of sulfur melt or low sulfur vapour pressure as employed in this study represents an advantaged condition for generating the nano-sulfur by physical vapour deposition. The nanostructured sulfur and sulfur nano-hybrids may have significant application in energy storage, catalyst and so on.

The authors gratefully acknowledge the financial support from Washington State University Research Advancement Challenge (RAC) grant and NSF CMMI 1463616. The authors also gratefully acknowledge the support on morphology characterizations from the Franceschi Microscopy & Imaging Center. Moreover, the authors thank Dr. Arda Gozen and Mr. Sepehr Nesaei (Washington State University) for the help with the measurement of the temperature.

Notes and references

1. Y. X. Yin, S. Xin, Y. G. Guo and L. J. Wan, *Angew Chem-Int Edit*, 2013, **52**, 13186-13200.
2. Y. Yang, G. Y. Zheng and Y. Cui, *Chem Soc Rev*, 2013, **4**, 3018-3032.
3. P. G. Bruce, S. A. Freunberger, L. J. Hardwick and J. M. Tarascon, *Nat Mater*, 2012, **11**, 19-29.
4. W. J. Chung, J. J. Griebel, E. T. Kim, H. Yoon, A. G. Simmonds, H. J. Ji, P. T. Dirlam, R. S. Glass, J. J. Wie, N. A. Nguyen, B. W. Guralnick, J. Park, A. Somogyi, P. Theato, M. E. Mackay, Y. E. Sung, K. Char and J. Pyun, *Nat Chem*, 2013, **5**, 518-524.
5. G. Y. Zheng, Y. Yang, J. J. Cha, S. S. Hong and Y. Cui, *Nano Lett*, 2011, **11**, 4462-4467.
6. A. Manthiram, Y. Z. Fu and Y. S. Su, *Acc Chem Res*, 2013, **46**, 1125-1134.
7. L. Ma, H. L. Zhuang, Y. Y. Lu, S. S. Moganty, R. G. Hennig and L. A. Archer, *Adv Energy Mater*, 2014, **4**.
8. G. Liu, P. Niu, L. C. Yin and H. M. Cheng, *J Am Chem Soc*, 2012, **134**, 9070-9073.
9. G. Liu, P. Niu and H. M. Cheng, *Chemphyschem*, 2013, **14**, 885-892.
10. H. W. Chen, C. H. Wang, W. L. Dong, W. Lu, Z. L. Du and L. W. Chen, *Nano Lett*, 2015, **15**, 798-802.
11. H. W. Chen, W. L. Dong, J. Ge, C. H. Wang, X. D. Wu, W. Lu and L. W. Chen, *Sci Rep-Uk*, 2013, **3**.
12. W. Y. Li, G. Y. Zheng, Y. Yang, Z. W. Seh, N. Liu and Y. Cui, *P Natl Acad Sci USA*, 2013, **110**, 7148-7153.
13. C. Y. Hu, S. Z. Zheng, C. J. Lian, F. Chen, T. W. Lu, Q. H. Hu, W. W. Duo, R. B. Zhang and C. Y. Guan, *J Mol Catal a-Chem*, 2015, **396**, 128-135.
14. K. J. Rao and S. Paria, *Rsc Adv*, 2013, **3**, 10471-10478.
15. T. Schneider, A. Baldauf, L. A. Ba, V. Jamier, K. Khairan, M.-. Sarakbi, N. Reum, M. Schneider, A. Roeseler, K. Becker, T. Burkholz, P. G. Winyard, M. Kelkel, M. Diederich and . Jacob, *Journal of Biomedical Nanotechnology*, 2011, **7**, 395-405.
16. K. Ghanemi, Y. Nikpour, O. Omidvar and A. Maryamabadi, *Talanta*, 2011, **85**, 763-769.
17. D. Bresser, S. Passerini and B. Scrosati, *Chem Commun*, 2013, **49**, 10545-10562.
18. L. Chen and L. L. Shaw, *J Power Sources*, 2014, **267**, 770-781.
19. A. S. Deshpande, R. B. Khomane, B. K. Vaidya, R. M. Joshi, A. S. Harle and B. D. Kulkarni, *Nanoscale Res Lett*, 2008, **3**, 221-229.
20. Y. M. Guo, J. Z. Zhao, S. F. Yang, Z. C. Wang and H. B. Zhang, *Powder Technol*, 2006, **162**, 83-86.
21. I. A. Massalimov, A. R. Shainurova, A. N. Khusainov and A. G. Mustafin, *Russ J Appl Chem+*, 2012, **85**, 1832-1837.
22. Y. M. Guo, Y. H. Deng, J. Z. Zhao, Z. C. Wang and H. B. Zhang, *Acta Chim. Sin.*, 2005, **63**, 337-340.
23. R. G. Chaudhuri and S. Paria, *J Colloid Interf Sci*, 2010, **343**, 439-446.
24. B. Meyer, *Chem Rev*, 1976, **76**, 367-388.